OPEN ACCESS Freely available online

PLOS ONE

Mechanisms of a Human Skeletal Myotonia Produced by Mutation in the C-Terminus of $Na_V1.4$: Is Ca^{2+} Regulation Defective?

Subrata Biswas, Deborah A. DiSilvestre, Peihong Dong, Gordon F. Tomaselli*

Department of Medicine, Division of Cardiology, Johns Hopkins University, Baltimore, Maryland, United States of America

Abstract

Mutations in the cytoplasmic tail (CT) of voltage gated sodium channels cause a spectrum of inherited diseases of cellular excitability, yet to date only one mutation in the CT of the human skeletal muscle voltage gated sodium channel ($hNa_V1.4_{F1705I}$) has been linked to cold aggravated myotonia. The functional effects of altered regulation of $hNa_V1.4_{F1705I}$ are incompletely understood. The location of the $hNa_V1.4_{F1705I}$ in the CT prompted us to examine the role of Ca^{2+} and calmodulin (CaM) regulation in the manifestations of myotonia. To study Na channel related mechanisms of myotonia we exploited the differences in rat and human $Na_V1.4$ channel regulation by Ca^{2+} and CaM. $hNa_V1.4_{F1705I}$ inactivation gating is Ca^{2+}-sensitive compared to wild type $hNa_V1.4$ which is Ca^{2+} insensitive and the mutant channel exhibits a depolarizing shift of the $V_{1/2}$ of inactivation with CaM over expression. In contrast the same mutation in the $rNa_V1.4$ channel background ($rNa_V1.4_{F1698I}$) eliminates Ca^{2+} sensitivity of gating without affecting the CaM over expression induced hyperpolarizing shift in steady-state inactivation. The differences in the Ca^{2+} sensitivity of gating between wild type and mutant human and rat $Na_V1.4$ channels are in part mediated by a divergence in the amino acid sequence in the EF hand like (EFL) region of the CT. Thus the composition of the EFL region contributes to the species differences in Ca^{2+}/CaM regulation of the mutant channels that produce myotonia. The myotonia mutation F1705I slows I_{Na} decay in a Ca^{2+}-sensitive fashion. The combination of the altered voltage dependence and kinetics of I_{Na} decay contribute to the myotonic phenotype and may involve the Ca^{2+}-sensing apparatus in the CT of $Na_V1.4$.

Citation: Biswas S, DiSilvestre DA, Dong P, Tomaselli GF (2013) Mechanisms of a Human Skeletal Myotonia Produced by Mutation in the C-Terminus of $Na_V1.4$: Is Ca^{2+} Regulation Defective? PLoS ONE 8(12): e81063. doi:10.1371/journal.pone.0081063

Editor: Alexander G. Obukhov, Indiana University School of Medicine, United States of America

Received July 10, 2013; **Accepted** October 8, 2013; **Published** December 6, 2013

Funding: This study was supported by the National Institutes of Health (RO1HL50411 to Dr. Gordon F. Tomaselli). No additional external funding received for this study. The funders had no role in study design, data collection and analysis, decision to publish, or preparation of the manuscript.

Competing Interests: The authors have declared that no competing interests exist.

* E-mail: gtomasel@jhmi.edu

Introduction

Precise and coordinated activity of skeletal muscle results from highly regulated signals generated by the orchestrated activities of different ion channels. A spectrum of muscle disorders are caused by the mutations in different ion channels [1]. A number of mutations in different regions of the human voltage-gated Na channel, $hNa_V1.4$ have been reported to cause skeletal muscle disorders [2]. Mutations in the transmembrane domains and linker regions cause cold aggravated myotonia [3,4,5,6] yet only one case of cold aggravated myotonia [7], has been linked to a mutation in the CT of the skeletal muscle sodium channel, $hNa_V1.4$ (F1705I, Figure 1A) and functionally studied. The other mutation in the CT-$Na_V1.4$, E1702K has been linked to paramyotonia congenita [8], but not functionally studied. Interestingly, another mutation Q1633E, causes potassium aggravated myotonia and is located in the EF hand like (EFL) region, that is the region in and around Helix 1, and the loop between Helix 1 and Helix 2 of the CT-$hNa_V1.4$, and about 71 amino acids upstream of the E1705I mutation. Q1633E and F1705I have comparable electrophysiological effects including disruption of fast inactivation, slowed current decay, and a depolarized shift in the voltage dependence of availability [9]. $hNa_V1.4$ mutations that cause myotonic disorders are associated with changes in the kinetics and voltage dependence of gating generally resulting in a gain-of-function.

There is substantial evidence that the CT of Na_V channels regulate the kinetics and voltage dependence of inactivation [10,11,12,13]. Moreover, Ca^{2+} and CaM/CaM kinase (CaMK) distinctly modulate inactivation of different isoforms of Na_V channels through interaction with structural motifs in the CT although the mechanisms are not fully understood [10,11,14,15,16,17,18]. There is evidence, particularly in HEK cells, that over expression of CaM will alter $Na_V1.4$ channel gating [10,15,16], and this is not unique to this channel but it also observed for other voltage dependent channels [15,19,20]. An EFL sequence [21,22] in the CT of $Na_V1.5$ and $Na_V1.1$ has been shown to influence Ca^{2+} regulation of channel gating [14,17,18,23,24,25]. Other acidic residues in the H1–H2 loop of the proximal C-terminus may affect Ca^{2+} sensitivity of channel gating as well [24,26], and the NMR solution and crystal structures in this region reveals binding of Ca^{2+} [24] or Mg^{2+} [27]. In addition to the EFL, sites in the III–IV linker are involved in Ca^{2+}/CaM mediated regulation of gating [28,29,30]. Similar Ca^{2+}/CaM sites are also present in the CT of $Na_V1.4$; however, their roles in channel regulation and relevance to disease causing mutations of the CT-$Na_V1.4$ are not known. The goals of this

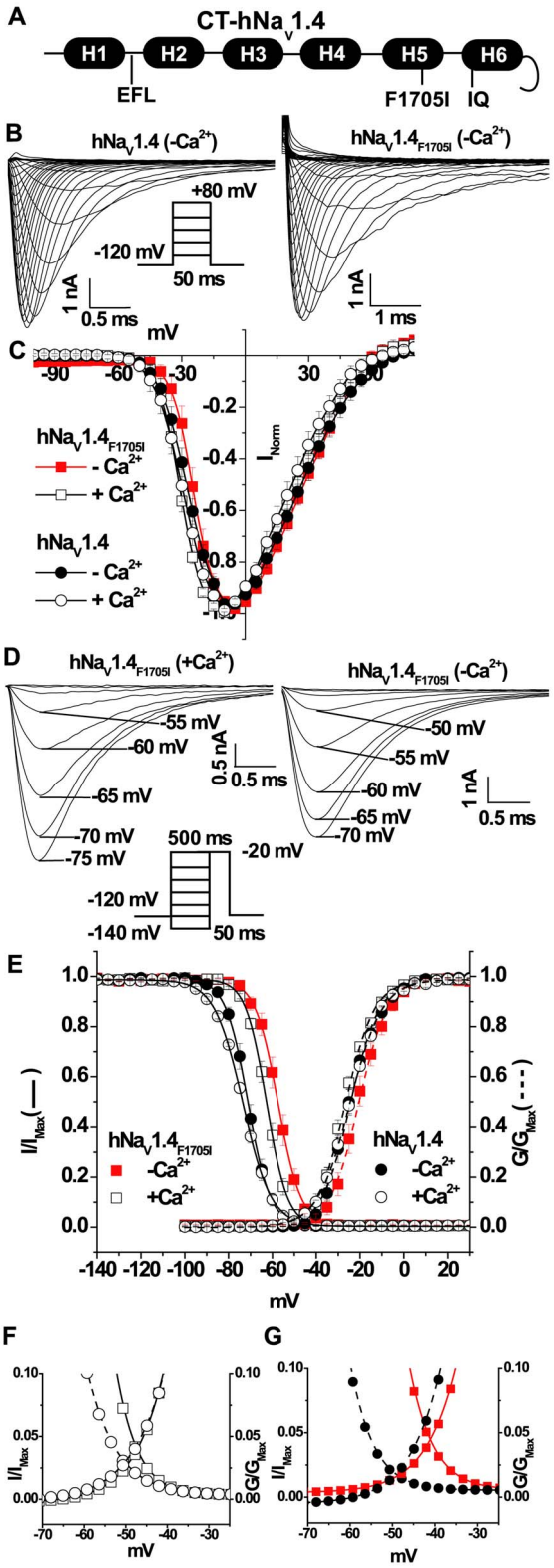

Figure 1. Ca^{2+}-sensitivity of human $Na_V1.4_{F1705I}$ inactivation. (**A**) A schematic of the structured region of the C-terminus of $hNa_V1.4$ between amino acids residues 1788 and 2040, the predicted helices are labeled H1–H6. The location of the EFL residues in and around H1 harbors species specific variations in the key Ca^{2+} sensing residues in $hNa_V1.4$ (G1613S and A1636D) compared with the rat isoform. The CaM binding motif IQ in H6 and, the cold aggravated myotonia mutation F1705I (rat: F1698I) in H5 are illustrated. (**B**) Representative whole-cell currents through wild type and mutant $hNa_V1.4_{F1705I}$ channels expressed in HEK293 cells in $[Ca^{2+}]_i$ free conditions. Na^+ currents were elicited by the protocol in the inset. (**C**) $[Ca^{2+}]_i$ does not alter the I–V relationship of $hNa_V1.4_{F1705I}$. (**D**) Representative steady-state inactivation currents from different holding potentials through mutant $hNa_V1.4_{F1705I}$ channels in the presence of 0.5 μM or absence of Ca^{2+}. (**E**) Activation and steady-state inactivation curves of wild type and $hNa_V1.4_{F1705I}$ channels in the absence and presence of 0.5 μM intracellular Ca^{2+}. The $V_{1/2}$ of inactivation of $hNa_V1.4_{F1705I}$ is sensitive to $[Ca^{2+}]_i$ and significantly shifted in the hyperpolarizing direction in the presence of Ca^{2+} ($p<0.005$). The activation relationships are fitted with dotted lines, the $V_{1/2}$ of activation are unaffected by change in $[Ca^{2+}]_i$. (**F**) and (**G**) illustrate the window currents through wild type and $hNa_V1.4_{F1705I}$ in presence (**F**) and absence (**G**) of intracellular Ca^{2+}, respectively. Dotted lines represent the wild type channel. The symbols and color are the same in plots C, E, F, and G.
doi:10.1371/journal.pone.0081063.g001

study are to understand the pathogenesis of temperature sensitive myotonia caused by the F1705I mutation, and to use this naturally occurring mutation (and the species specific differences) to better understand the regulation of the Na_V channels by Ca^{2+}. We demonstrate that the $hNa_V1.4_{F1705I}$ alters the voltage dependence of inactivation and the temperature sensitivity of current kinetics. In addition, key residues in the EFL alter the CaM and Ca^{2+} dependence of channel gating which may also contribute to the myotonia phenotype.

Materials and Methods

Plasmid Construction

The EYFP fused channel construct $Na_V1.4$-EYFP was prepared as described previously [15]. The myotonia causing mutation in the rat CT, $rNa_V1.4_{F1698I}$, was made by site directed mutagenesis using primer pairs:

Forward (F): 5′CATGGAGGAGAAGATTATGGCAGCTAACCCTTC3′ and

Reverse (R): 5′GAAGGGTTAGCTGCCATAATCTTCTCCTCCATG3′. The human myotonia construct, $hNa_V1.4_{F1705I,}$ was made by site directed mutagenesis of the human $hNa_V1.4$-EYFP construct using primer pairs:

Forward (F): 5′ CATGGAGGAGAAGATCATGGCAGCCAAC3′ and $hNa_V1.4_{F1705I}$ Reverse (R): 5′ GTTGGCTGCCATGA*TCT*TCTCCTCCATG3′. All the clones were sequence verified.

Transfection of Cells

Approximately 0.75×10^6 Human embryonic kidney cells (HEK293; American Type Culture Collection, Manassas, VA) were cultured in 6-well tissue culture dishes in DMEM supplemented with 10% FBS, L-glutamine (2 mmol/L), penicillin

Table 1. Biophysical characteristics of $Na_V1.4$ variants.

Channel/Mutant		Steady-state inactivation	Activation	τ_{Rec}
		$V_{1/2}$ (mV)	$V_{1/2}$ (mV)	(ms)
$rNa_V1.4$	$+Ca^{2+}$	−64.2±0.1(7)	−29.0±0.3(6)	2.3±0.1(7)
	$-Ca^{2+}$	−72±0.1(11)[a]	−31±1.5(13)	2.5±0.3(5)
$rNa_V1.4$	CaM	−69.3±0.1(5)[a]	−30.6±0.2(6)	2.2±0.1(10)
(0.5 μM Ca^{2+})	CaM_{1234}	−64.3±0.3(6)	−29.4±0.3(6)	2.6±0.1(5)
$rNa_V1.4_{F1698I}$	$+Ca^{2+}$	−49.7±0.5(6)[a]	−16.6±1(6)[a]	1.7±0.1(5)
	$-Ca^{2+}$	−49.7±0.8(9)	−15.3±1.3(7)	1.5±0.2(6)
$rNa_V1.4_{F1698I}$	CaM	−54.7±0.6(11)[b]	−17.9±0.7(9)	2.6±0.3(9)
(0.5 μM Ca^{2+})	CaM_{1234}	−47.9±1.9(6)	−18.7±2(8)	3±0.3(5)
$rNa_V1.4_{SD/GA}$	$+Ca^{2+}$	−70.0±0.2(8)[a]	−18.9±0.3(5)	2.3±0.1(8)
	$-Ca^{2+}$	−70.4±0.2(6)	−19.0±0.3(6)	2.0±0.1(5)
$rNa_V1.4_{SD/GA}$	CaM	−62.9±0.1(6)[c]	−20.8±0.3(5)	2.9±0.1(6)
(0.5 μM Ca^{2+})	CaM_{1234}	−64.1±0.1(8)[c]	−19.0±0.4(9)	2.3±0.1(9)
$rNa_V1.4_{F1698I+SD/GA}$	$+Ca^{2+}$	−62.9±0.1(8)	−26±0.2(6)	2.1±0.1(8)
	$-Ca^{2+}$	−57.3±0.1(5)[d]	−28.6±0.2(5)	2.0±0.1(5)
$rNa_V1.4_{F1698I+SD/GA}$	CaM	−51.5±0.1(6)[d]	−21.4±0.3(6)	2.3±0.1(7)
(0.5 μM Ca^{2+})	CaM_{1234}	−52.9±0.1(5)[d]	−22.9±0.3(5)	2.1±0.1(6)
$hNa_V1.4$	$+Ca^{2+}$	−73.5±0.1(9)	−23±0.1(8)	2.4±0.1(6)
	$-Ca^{2+}$	−71.2±0.1(7)	−24.4±0.3(5)	1.9±0.1(5)
$hNa_V1.4$	CaM	−63.8±0.1(7)[e]	−15.4±0.2(6)[e]	2.8±0.1(5)
(0.5 μM Ca^{2+})	CaM_{1234}	−65.1±0.1(6)[e]	−15.5±0.2(5)[e]	2.9±0.1(6)
$hNa_V1.4$	CaM	−80.4±0.2(5)[f]	−15.5±0.2(5)	3.3±0.1(5)
(0 Ca^{2+})	CaM_{1234}	−72.1±0.2(5)	−15.5±0.2(5)	2.4±0.1(5)
$hNa_V1.4_{F1705I}$	$+Ca^{2+}$	−62.7±0.1(5)[e1]	−24.6±0.3(5)	1.7±0.1(5)
	$-Ca^{2+}$	−57.5±0.1(7)[g]	−23±0.2(7)	3.1±0.1(5)
$hNa_V1.4_{F1705I}$	CaM	−56.8±0.1(5)[g]	−22.7±0.1(6)	2.7±0.1(5)
(0.5 μM Ca^{2+})	CaM_{1234}	−52.4±0.1(5)[g]	−21.7±0.1(5)	2.2±0.1(5)
$hNa_V1.4_{F1705I}$	CaM	−61.7±0.1(5)	−22.9±0.1(6)	2.8±0.(3)
(0 Ca^{2+})	CaM_{1234}	−60.4±0.5(5)	−21.7±0.1(5)	2.8±0.2(3)
$hNa_V1.4_{GS/AD}$	$+Ca^{2+}$	−62.2±0.1(6)[e]	−19.8±0.2(6)	2.3±0.1(6)
	$-Ca^{2+}$	−67.2±0.1(7)[h]	−16.0±0.2(8)	2.7±0.1(5)
$hNa_V1.4_{GS/AD}$	CaM	−70.2±0.1(5)[h1]	−20.5±0.2(6)	3.4±0.1(5)
(0.5 μM Ca^{2+})	CaM_{1234}	−65.3±0.1(5)	−18±0.2(5)	3.3±0.2(5)
$hNa_V1.4_{F1705I+GS/AD}$	$+Ca^{2+}$	−54.8±0.1(6)[g]	−23.3±0.3(6)	3.1±0.2(5)
	$-Ca^{2+}$	−53.9±0.1(5)	−24.2±0.2(5)	2.4±0.1(5)
$hNa_V1.4_{F1705I+GS/AD}$	CaM	−59.3±0.1(5)[i]	−21.2±0.2(5)	2.7±0.1(5)
(0.5 μM Ca^{2+})	CaM_{1234}	−56.8±0.1(7)	−20.3±0.3(9)	3.2±0.1(6)

Values: Mean±S.E(n); $+Ca^{2+}$ = 0.5 μM Ca^{2+}:
[a]vs. $rNa_V1.4$ (0.5 μM Ca^{2+});
[b]vs. $rNa_V1.4_{F1698I}$ (0.5 μM Ca^{2+});
[c]vs. $rNa_V1.4_{SD/GA}$ (0.5 μM Ca^{2+});
[d]vs. $rNa_V1.4_{F1698I+SD/GA}$ (0.5 μM Ca^{2+});
[e]vs. $hNa_V1.4$ (0.5 μM Ca^{2+});
[e1]vs. $hNa_V1.4$ (0.5 μM Ca^{2+});
[f]vs. $hNa_V1.4$ (0 and 0.5 μM Ca^{2+});
[g]vs. $hNa_V1.4_{F1705I}$ (0.5 μM Ca^{2+});
[h]vs. $hNa_V1.4_{GS/AD}$ (0.5 μM Ca^{2+});
[h1]vs. $hNa_V1.4_{GS/AD}$ (0.5 μM Ca^{2+});
[i]vs. $hNa_V1.4_{F1705I+GS/AD}$ (0.5 μM Ca^{2+}).
doi:10.1371/journal.pone.0081063.t001

(100 U/mL), and streptomycin (10 mg/mL). The cells were co-transfected with plasmids encoding the β1 subunit and the appropriate fluorescently–tagged $Na_V1.4$ and CaM variants: human or rat wild type $Na_V1.4$-EYFP, $hNa_V1.4_{F1705I}$-EYFP, $rNa_V1.4_{F1698I}$-EYFP, $hNa_V1.4_{F1705I+GA/SD}$-EYFP and ECFP-CaM or ECFP-CaM_{1234} alone or in combination. Cells were

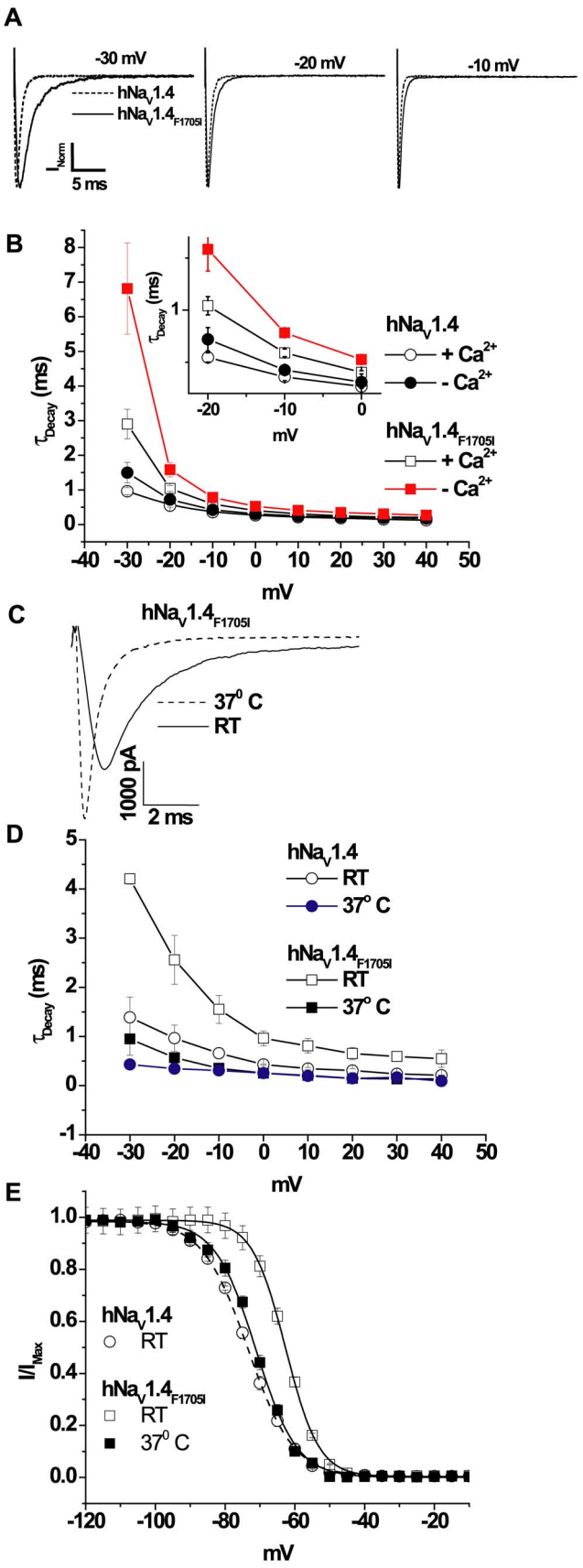

Figure 2. Current decay of myotonia mutant channels. The time constant of decay is altered in $hNa_V1.4_{F1705I}$ compared to wild type $hNa_V1.4$ channels. (**A**) Superimposed normalized currents through wild type and $hNa_V1.4_{F1705I}$ channels at test pulses of −30, −20, and −10 mV exhibiting slowing of current decay in the mutant channel. (**B**) The time constants of current decay of $hNa_V1.4_{F1705I}$ channels are significantly different compared to wild type in the absence ($p<0.05$) or presence of 0.5 μM of Ca^{2+} ($p<0.001$). The inset is an expanded view −20 mV to 0 mV. (**C**) Raw current traces of $hNa_V1.4_{F1705I}$ channels at RT and at 37°C. Currents were measured at −20 mV, in the same cell at different temperatures with 0.5 μM of Ca^{2+} in the pipette. (**D**) Plot of the time constants of current decay of wild type and $hNa_V1.4_{F1705I}$ channels at RT and at 37°C in 0.5 μM of Ca^{2+}. Paired measurements were made at RT and at 37°C. The current decay of $hNa_V1.4_{F1705I}$ is significantly different at 37°C compared to RT ($p<0.05$). (**E**) Plot of the steady-state inactivation of $hNa_V1.4_{F1705I}$ channels at 37°C in 0.5 μM of Ca^{2+}. For comparison the steady-state inactivation of wild type and $hNa_V1.4_{F1705I}$ from Figure 1E are re-plotted. The symbols are the same in plots B, D and E.
doi:10.1371/journal.pone.0081063.g002

transfected using Lipofectamine™ 2000 (Invitrogen) according to the manufacturer's instructions and were studied 48 to 72 hours post-transfection. The total amount of DNA for all transfections was kept constant.

Electrophysiology

HEK293 cells expressing wild type or mutant EYFP-tagged $Na_V1.4$ channels were selected for recording. In some experiments, cells expressing both yellow and cyan fluorophores that were co-transfected with tagged $Na_V1.4$ channel variants and CaM or CaM_{1234} were selected for patching. Cells were patch clamped with an Axopatch 200B patch-clamp amplifier using pipettes with tip resistances of 1–3 MΩ and typical series resistance compensation of >90% to minimize voltage clamp errors. Current recording was initiated 10 minutes after establishing whole-cell configuration, and currents were filtered at 5 kHz.

All the solutions used in this study were prepared as described previously [14,17,31,32]. The bath solution contained (in mmol/L): 145 NaCl, 4 KCl, 1.8 $CaCl_2$, 1 $MgCl_2$, 10 glucose and 10 Na-HEPES (pH 7.4). The Ca^{2+} free patch pipette solution contained (in mmol/L): 10 NaF, 100 CsF, 20 $CsCl_2$, 20 BAPTA, 0 $CaCl_2$ and 10 HEPES, pH adjusted to 7.35 with CsOH. The 0.5 μmol/L Ca^{2+} patch pipette solution contained (in mmol/L): 10 NaF, 100 CsF, 20 $CsCl_2$, 5 BAPTA, 4 $CaCl_2$ and 10 HEPES, pH adjusted to 7.35 with CsOH. The osmolarity of the bath and pipette solutions were equalized using glucose. The free [Ca^{2+}] in the solutions was estimated with WEBMAX Standard software (http://www.stanford.edu/~cpatton/webmaxcS.htm) and found to be about 0.5 μM. The free [Ca^{2+}] in the solutions was verified by measurement using a Kwik-Tip Calcium ion-selective electrode (WPI) (Figure S1 and Table S1 in File S1). We studied the effect of intracellular Ca^{2+} on the voltage dependence of inactivation gating of $rNa_V1.4$ with chloride substituted for fluoride in the pipette solution and found no significant difference in the Ca^{2+} sensitivity of gating (Figure S2 in File S1).

Standard two-pulse protocols were used to generate the steady-state inactivation curves. The voltage dependence of steady-state fast inactivation was studied using 500 ms inactivation pre-pulses over a voltage range from −140 to +30 mV in steps of 5 mV, followed by a 50 ms test pulse at −20 mV. Currents were normalized to the maximal current (I_{max}) and fit to a Boltzmann function of the form $(y = [(A_1-A_2)/(1+e^{(x-x0)/dx})]+A_2)$ to determine the membrane potential eliciting half-maximal inactivation ($V_{1/2}$), where A_1 and A_2 are maximum and minimum availabil-

Table 2. Na current decay time constants of $hNa_V1.4$ and myotonia mutant $hNa_V1.4_{F1705I}$.

Channel/Mutant		τ_{Decay} (ms)			
		−30 mV	−20 mV	−10 mV	0 mV
$hNa_V1.4$	0.5 μM Ca^{2+}	0.96±0.1(8)	0.54±0.05(8)	0.36±0.04(8)	0.26±0.02(8)
	Ca^{2+} free	1.5±0.3(5)	0.71±0.11(5)	0.42±0.05(5)	0.3±0.02(5)
	37°C (0.5 μM Ca^{2+})	0.43±0.01(5)	0.35±0.01(5)	0.3±0.02(5)	0.25±0.02(5)
$hNa_V1.4_{F1705I}$	0.5 μM Ca^{2+}	2.9±0.4(5)$^{\#}$	1.04±0.09(5)$^{\#}$	0.59±0.03(5)$^{\#}$	0.4±0.01(5)$^{\#}$
	Ca^{2+} free	6.8±1.3(7)$^{\%}$	1.6±0.2(7)$^{\$}$	0.78±0.03(7)$^{\$}$	0.52±0.03(7)$^{\$}$
	37°C (0.5 μM Ca^{2+})	0.95±0.3(5)*@	0.56±0.1(5)*	0.35±0.01(5)*	0.25±0.01(5)*

Values: Mean±S.E(n);
$^{\#}$vs. $hNa_V1.4$ in 0.5 μM Ca^{2+};
$^{\%}$vs. $hNa_V1.4_{F1705I}$ (0.5 μM Ca^{2+});
$^{\$}$vs. $hNa_V1.4_{F1705I}$ (0.5 μM Ca^{2+});
@vs. hNaV1.4 (37°C, 0.5 μM Ca2+);
*vs. $hNa_V1.4_{F1705I}$ (0.5 μM Ca^{2+}).
doi:10.1371/journal.pone.0081063.t002

ities, respectively, x0 is equivalent to $V_{1/2}$, and dx represents the slope factor. Activation curves were generated from a family of 50 ms test pulses from −100 mV to +80 mV in 5 mV increments from a holding potential of −120 mV. Peak currents at each membrane potential normalized to $I_{max,}$ were plotted to generate the I–V curves. Conductance (G) was calculated for peak current (I_{Peak}) at each membrane potential (V_m) using the equation ($G = I_{Peak}/(V_m - V_{Reversal})$). G was normalized to G_{Max} and fitted to a Boltzmann distribution to determine the membrane potential eliciting half-maximal activation ($V_{1/2}$). Deactivation was assessed using tail currents elicited by a test pulse of 0.5 ms to +40 mV followed by repolarization to a family of voltages ranging from −180 to −50 mV. I_{Na} decay rates were assessed by fitting to a single exponential decay (Figure S3 in File S1). Recovery from inactivation was assessed by a standard two-pulse protocol with a first pulse duration of 30 ms and a second pulse of 30 ms to −20 mV with varying inter pulse intervals from 1 to 200 ms at −120 mV. Exponential functions of the form $y = y0 + Ae^{-x/\tau}$ were fitted to recovery data to determine time constants (τ_{rec}), where y0 is the offset and A is amplitude. Significance was assessed using unpaired student's t-test (Microcal Origin, Microcal Software Inc. MA), and $p<0.05$ was considered significant.

Results

$hNa_V1.4_{F1705I}$ Alters Current Kinetics and Gating

A mutation (F1705I) in the structured portion of the CT of $hNa_V1.4$ has been associated with cold aggravated myotonia (Figure 1A). We studied the effect of $hNa_V1.4_{F1705I}$ on channel function by transient expression in HEK293 cells at RT. Currents through wild type $hNa_V1.4$ and $hNa_V1.4_{F1705I}$ channels were elicited by a family of depolarizing pulses ranging from −100 mV to +80 mV from a holding potential of −120 mV (Inset Figure 1B). The normalized peak current-voltage (I–V) relationships of wild type $hNa_V1.4$ and $hNa_V1.4_{F11705I}$ were not different in 0.5 μM $[Ca^{2+}]_i$ mimicking the average intracellular $[Ca^{2+}]$ in muscle (Figure 1B and 1C). The voltage dependence ($V_{1/2}$) of activation of the wild type and mutant channels did not differ in the presence of 0.5 μM $[Ca^{2+}]_i$ (Figure 1E and Table 1).

The voltage dependence of steady-state inactivation was altered by $hNa_V1.4_{F1705I}$. Compared to the wild type channel, the $V_{1/2}$ of the steady-state inactivation curve of $hNa_V1.4_{F1705I}$ was significantly shifted ∼+11 mV in 0.5 μM $[Ca^{2+}]_i$ ($V_{1/2}$ $hNa_V1.4$: −73.5±0.1 mV and $V_{1/2}$ $hNa_V1.4_{F1705I}$: −62.7±0.1 mV, $p<0.001$; Figure 1E and Table 1). In the absence of a significant shift in the activation curve this produces a significant increase in the window current of $hNa_V1.4_{F1705I}$ compared to wild type $hNa_V1.4$ in the presence or absence of $[Ca^{2+}]_i$ (Figures 1F and 1G). Thus, $hNa_V1.4_{F1705I}$ destabilizes steady-state inactivation and increases window current; however, the mechanism by which the mutation produces altered voltage dependence of gating is unknown. Given the importance of the CT of Na_V channels in the regulation of gating by Ca^{2+}/CaM signaling we assessed whether $hNa_V1.4_{F1705I}$ interfered with channel modulation by Ca^{2+} or CaM.

$hNa_V1.4_{F1705I}$ Alters Ca^{2+} Sensitivity

Intracellular Ca^{2+} has been shown to regulate the cardiac isoform of Na_V channels, $Na_V1.5$. It is not yet known if $[Ca^{2+}]_i$ similarly regulates skeletal muscle $Na_V1.4$ channels and if mutations in the CT of the channel affect Ca^{2+} regulation. In order to understand Ca^{2+} mediated regulation of $hNa_V1.4$ and $hNa_V1.4_{F1705I}$ we measured Na^+ currents with 20 mM BAPTA in the pipette solution to create the Ca^{2+}-free intracellular condition. The I–V relationships of wild type $hNa_V1.4$ and $hNa_V1.4_{F1705I}$ are almost identical (Figure 1C); and the $V_{1/2}$s of the activation (G−V) curves were unchanged in the absence of Ca^{2+} (Figure 1E and Table 1). The decay rate of wild type $hNa_V1.4$ was insensitive to the intracellular $[Ca^{2+}]$. The decay of $hNa_V1.4_{F1705I}$ currents is up to 2.5 times slower in the absence of Ca^{2+} compared to 0.5 μM $[Ca^{2+}]_i$ (Figures 2A, 2B and Table 2). The decay of $hNa_V1.4_{F1705I}$ was significantly slower than wild type $hNa_V1.4$ at all negative voltages at RT in both low and 0.5 μM $[Ca^{2+}]_i$ (Figures 2A, 2B and Table 2). We studied the effect of $hNa_V1.4_{F1705I}$ on current decay at 37°C, as patients with the mutation do not exhibit myotonia at normal body temperature. In contrast to RT, at 37°C in 0.5 μM $[Ca^{2+}]_i$, the current decay of $hNa_V1.4_{F1705I}$ is markedly hastened (Figure 2C) and is not significantly different from wild type except at −30 mV (Figures 2C, and 2D, Table 2). At 37°C the $V_{1/2}$ of steady-state inactivation of $hNa_V1.4_{F1705I}$ was significantly shifted in hyperpolarizing direction compared to RT ($V_{1/2}$ at 37°C: −71.6±0.1 mV and $V_{1/2}$ at RT: −62.7±0.1 mV, $p<0.001$; Figure 2E). I_{Na} decay, particularly at negative voltages, results from both inactivation and deactivation. We found no significant difference in the rates of deactivation at voltages between −180 and −100 mV ($p<0.05$; Figure S3 in File

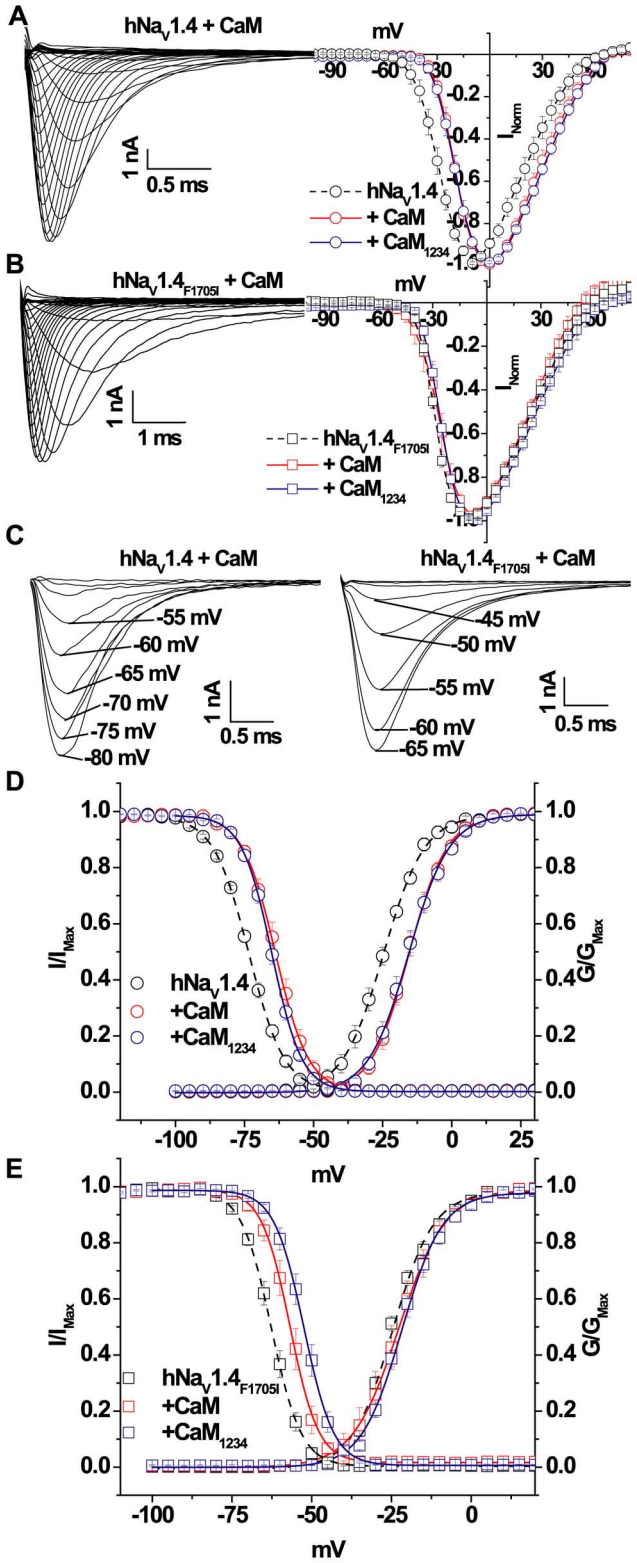

Figure 3. CaM-induced shift of inactivation in $hNa_V1.4$ channels. Representative Na^+ currents and I–V relationships for wild type (**A**) and $hNa_V1.4_{F1705I}$ channels (**B**) elicited by the same pulse protocol shown in the inset of Figure 1B. CaM and CaM_{1234} over expression significantly ($p<0.05$) shifts the wild type but not the $hNa_V1.4_{F1705I}$ I–V in the depolarizing direction. (**C**) Representative steady-state inactivation currents elicited from different holding potentials. (**D, E**) Plots of the steady-state inactivation and activation relationships of wild type $hNa_V1.4$ (**D**) and $hNa_V1.4_{F1705I}$ channels (**E**). The solid lines are the fits to steady-state inactivation data with CaM and CaM_{1234} over expression. There is a significant ($p<0.005$) depolarizing shift of the inactivation curve by CaM and CaM_{1234} compared to the expression of $hNa_V1.4_{F1705I}$ alone. The symbols and colors are the same in all panels of the figure.
doi:10.1371/journal.pone.0081063.g003

S1) similar to previous results [33]. However, at voltages from −90 mV to −60 mV, $\tau_{Deactivation}$ of $hNa_V1.4_{F1705I}$ in the Ca^{2+} free condition is significantly larger than in the wild type channel, with or without Ca^{2+} ($p<0.05$; Figure S3 in File S1).

Our previous work showed that the cardiac isoform $hNa_V1.5$ is $[Ca^{2+}]_i$ sensitive, and lowering intracellular Ca^{2+} shifts the $V_{1/2}$ of steady-state fast inactivation of $hNa_V1.5$ in hyperpolarizing direction [14]. However, $hNa_V1.4$ was insensitive to $[Ca^{2+}]_i$ and altering $[Ca^{2+}]_i$ does not significantly affect the voltage dependence of steady-state inactivation of wild type $hNa_V1.4$ channels (Figure 1E). In contrast, the $V_{1/2}$ of steady-state inactivation of $hNa_V1.4_{F1705I}$ was shifted significantly (~5 mV) in the depolarizing direction in the absence of intracellular Ca^{2+} compared with the 0.5 μM $[Ca^{2+}]_i$ (Figures1D, 1E and Table 1). Thus $hNa_V1.4_{F1705I}$ exhibits Ca^{2+} sensitivity of steady-state inactivation

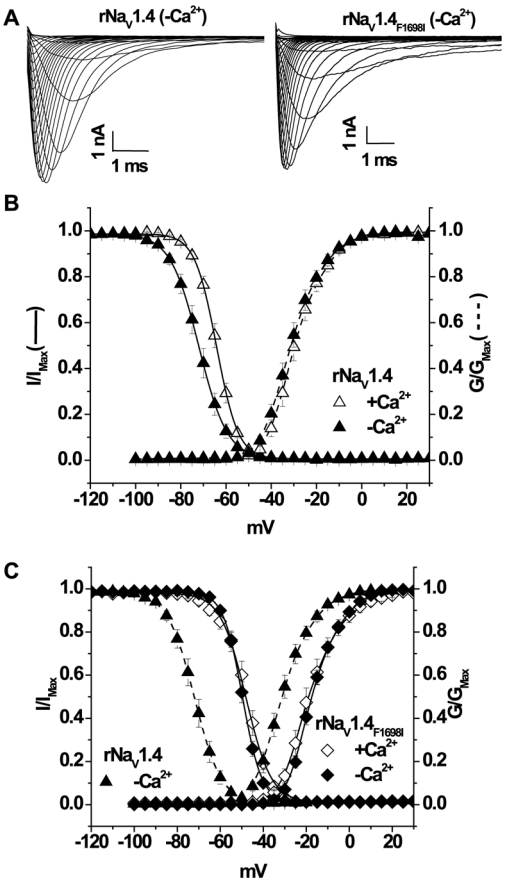

Figure 4. Ca^{2+} regulation of the rat $Na_V1.4$. Whole-cell $rNa_V1.4$ and $rNa_V1.4_{F1698I}$ expressed currents (**A**) are not affected by $[Ca^{2+}]_i$. (**B**) The voltage dependence of activation (dotted lines) and steady-state inactivation (solid lines) of $rNa_V1.4$. (**C**) $rNa_V1.4_{F1698I}$ significantly ($p<0.05$) shifts the activation and inactivation curves in the depolarizing direction and eliminates the sensitivity of inactivation to changes in $[Ca^{2+}]_i$. The dotted lines represent the wild type channel in the absence of $[Ca^{2+}]_i$. The symbols are the same in plots B and C.
doi:10.1371/journal.pone.0081063.g004

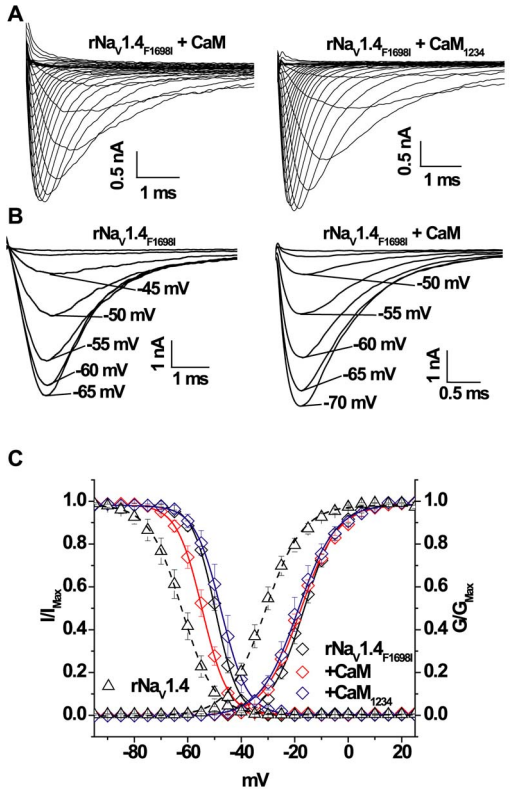

Figure 5. CaM shifts inactivation of rat $Na_V1.4_{F1698I}$. (**A**) Representative families of $rNa_V1.4_{F1698I}$ activation currents co-expressed with either CaM or CaM_{1234}. (**B**) Representative steady-state inactivation currents elicited from different holding potentials through $rNa_V1.4_{F1698I}$ channels in presence and absence of CaM over expression. (**C**) Activation and steady-state inactivation relationships. The solid lines are the fits to steady-state inactivation data of $rNa_V1.4_{F1698I}$ with CaM and CaM_{1234} over expression. There is a significant ($p<0.05$) shift of the inactivation curve by CaM compared to the expression of $rNa_V1.4_{F1698I}$ alone. Over expression of CaM_{1234} has no significant effect compared with the absence of CaM over expression. In contrast, the $V_{1/2}$ of activation of $rNa_V1.4_{F1698I}$, is not changed by co-expression of CaM or CaM_{1234}. The dotted lines in panel (**C**) represent wild type channel in 0.5 μM Ca^{2+}.
doi:10.1371/journal.pone.0081063.g005

distinct from wild type $hNa_V1.4$ which is insensitive to changes in $[Ca^{2+}]_i$.

$hNa_V1.4_{F1705I}$ Alters CaM Modulation

The F1705I mutation which is remote from the EFL region modifies the Ca^{2+} sensitivity of gating. F1705 is predicted to be in Helix 5 of the CT $hNa_V1.4$ and is closer in the linear amino acid sequence to the CaM binding IQ motif in Helix 6 (Figure 1A). Previously we have shown that CaM binds to the IQ motif and shifts the voltage dependence of inactivation of rat $Na_V1.4$ ($rNa_V1.4$) and Ca^{2+} binding-deficient $hNa_V1.5$ channels that are mutated in the EFL [10,14,15]. We tested the hypothesis that the large changes in Na^+ current inactivation exhibited by $hNa_V1.4_{F1705I}$ compared to wild type $hNa_V1.4$ are due to functional alterations in CaM interaction with the IQ motif. We examined the effects of CaM over expression on $hNa_V1.4_{F1705I}$ and wild type $hNa_V1.4$ gating. As Ca^{2+} can bind to CaM and modulate channel gating, we also studied effect of Ca^{2+} binding deficient CaM or apo-CaM (CaM_{1234}) to delineate direct effects of Ca^{2+} on the channel compared to Ca^{2+} effects through CaM. In contrast to the wild type rat $Na_V1.4$ channel [15], over expression of both CaM and CaM_{1234} with wild type human $Na_V1.4$ shifts the channel's I–V relation in the depolarizing direction in 0.5 μM $[Ca^{2+}]_i$ (Figure 3A and Table 1). Co-expression of CaM and CaM_{1234} with $hNa_V1.4$ significantly shifts the voltage dependence of activation in the depolarizing direction (Figure 3D). In contrast, neither the I–V relationships or voltage dependence of activation of $hNa_V1.4_{F1705I}$ were affected by co-expression with CaM or CaM_{1234} (Figures 3B, 3E and Table 1).

We previously demonstrated that CaM is tethered to the CT of $Na_V1.4$, and CaM binding to the IQ motif shifts the steady-state inactivation of the rat isoform in a hyperpolarizing direction [10,15] (Table 1). In contrast, co-expression of CaM with $hNa_V1.4$ significantly shifts wild type channel availability in the depolarizing direction in 0.5 μM $[Ca^{2+}]_i$ (Figures 3C and D) and in the hyperpolarizing direction in the Ca^{2+} free intracellular condition, when compared with the absence of exogenous CaM (Table 1; $p<0.05$). CaM_{1234} over expression in 0.5 μM $[Ca^{2+}]_i$ shifts the $V_{1/2}$ of inactivation of $hNa_V1.4$ in the depolarizing direction compared to the absence of CaM_{1234} (Figure 3D; $p<0.05$). Upon removal of $[Ca^{2+}]_i$, the $V_{1/2}$ of inactivation of $hNa_V1.4$ is not affected by CaM_{1234} over expression (Table 1; $p<0.05$). Co-expression of CaM or CaM_{1234} with the mutant, $hNa_V1.4_{F1705I}$ also significantly shifts channel availability in the depolarizing direction compared to the absence of CaM co-expression (Figures 3C, 3E and Table 1; $p<0.05$). Similar to wild type, in Ca^{2+} free conditions, CaM or CaM_{1234} co-expression shifts $V_{1/2}$ of steady-state inactivation in the hyperpolarizing direction (Table 1; $p<0.05$). Notably, in Ca^{2+} free conditions the CaM-induced hyperpolarizing shifts of steady-state inactivation of the wild type and mutant $hNa_V1.4$ channels are in same direction as in the rat $Na_V1.4$ channel.

We speculate that the difference in the voltage dependence of gating of wild type human and rat $Na_V1.4$ channels when co-expressed with Ca^{2+}-CaM/apo-CaM [15] may provide insights into the mechanisms of the Ca^{2+} modulation of channel function in the myotonia mutation and in wild type channels.

Effect of $rNa_V1.4_{F1698I}$ on Ca^{2+}/CaM Regulation of Channel Gating

The wild type rat and human isoforms of $Na_V1.4$ exhibit distinct differences in gating and regulation by Ca^{2+} and CaM. The orthologous mutation of $hNa_V1.4_{F1705I}$ in the rat is $rNa_V1.4_{F1698I}$. The activation curve of $rNa_V1.4_{F1698I}$ is significantly ($p<0.05$) shifted in the depolarizing direction (~+12 mV) compared to wild type $rNa_V1.4$ in 0.5 μM $[Ca^{2+}]_i$ (Figures 4A, 4B and Table 1). In contrast to $rNa_V1.4_{F1698I}$, no activation shift was seen with the F1705I mutation in human $Na_V1.4$ (Figure 1E). Similar shifts in the activation curves of other $Na_V1.4$ mutants that cause myotonia have previously been reported [34,35,36].

We next examined whether Ca^{2+} altered $rNa_V1.4_{F1698I}$ gating. The $V_{1/2}$s of the activation of both the wild type $rNa_V1.4$ and $rNa_V1.4_{F1698I}$ were not different in 0.5 μM Ca^{2+} compared with the absence of Ca^{2+} (Figures 4B, C and Table 1).

Unlike wild type $rNa_V1.4$, the voltage dependence of the steady-state inactivation of $rNa_V1.4_{F1698I}$ was not affected by the $[Ca^{2+}]_i$ (Figures 4B, 4C and Table 1). Neither $rNa_V1.4$ nor $rNa_V1.4_{F1698I}$ exhibit $[Ca^{2+}]_i$ sensitivity to recovery from inactivated states (Table 1). Thus the Ca^{2+} sensitivity of steady-state inactivation of $rNa_V1.4$ was eliminated with a mutation remote in the linear amino acid sequence from the EFL motif. Although the $rNa_V1.4_{F1698I}$ results in loss of Ca^{2+} sensitivity of the channel, it also dramatically affects steady-state inactivation of the channel producing approximately ~+15 mV shift of the $V_{1/2}$ compared to

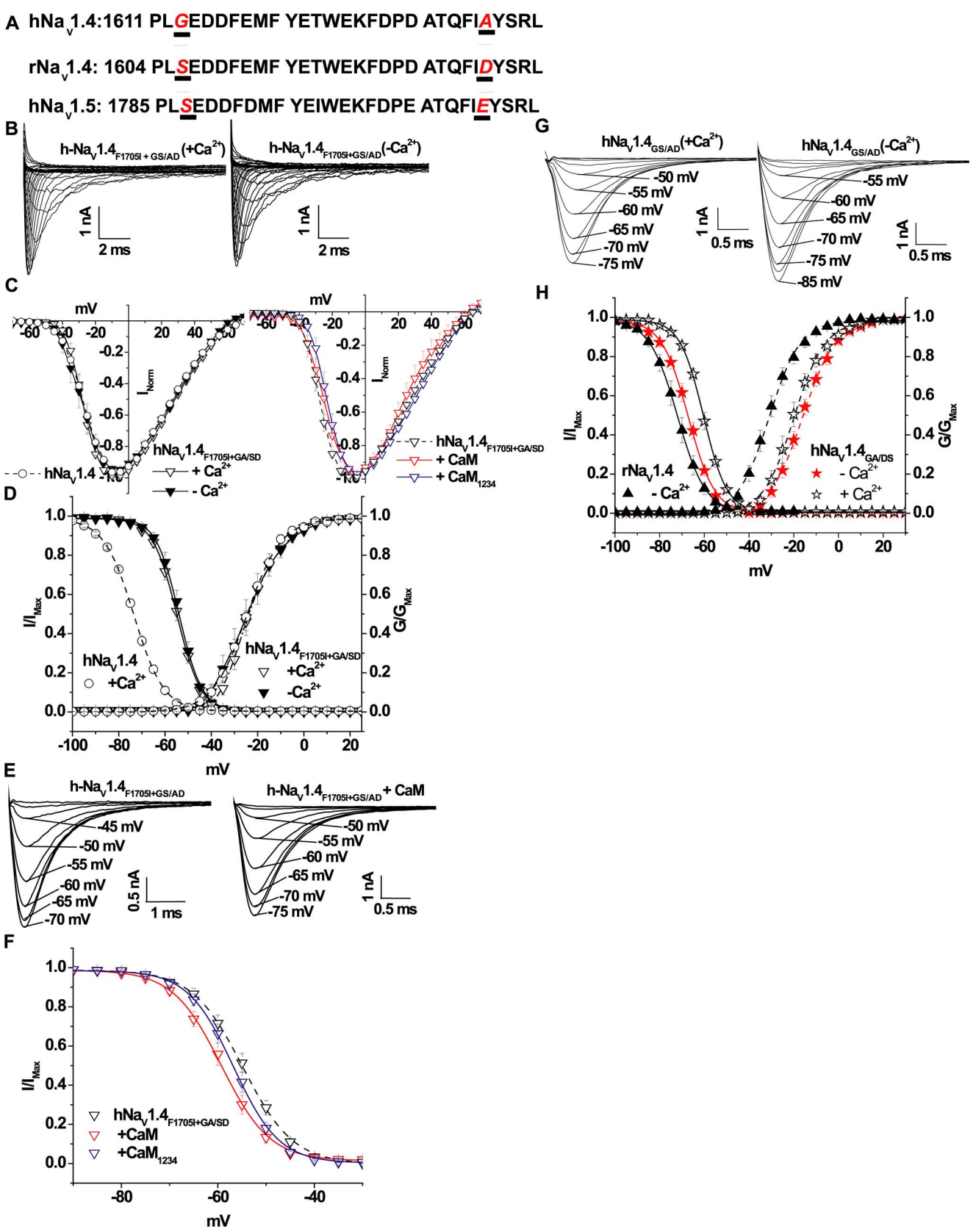

Figure 6. Exchange of human and rat EFL residues in hNa$_V$1.4. (**A**) Amino acid sequence alignment of the proximal CT of rat and human wild type Na$_V$1.4 channel and hNa$_V$1.5 demonstrate the similarity of rNa$_V$1.4 and hNa$_V$1.5 at key positions in the EFL. In hNa$_V$1.4$_{F1705I+GA/SD}$ residues G1613S and A1636D are substituted in the human channel hNa$_V$1.4$_{F1705I}$ to match the corresponding residues of rNa$_V$1.4. (**B**) Representative families of hNa$_V$1.4$_{F1705I+GA/SD}$ activation currents in the presence and absence of $[Ca^{2+}]_i$. (**C**) Normalized I–V relationships hNa$_V$1.4$_{F1705I+GA/SD}$ are not affected by

altered $[Ca^{2+}]_i$ or CaM and CaM_{1234} over expression. (**D**) The steady-state inactivation of $hNa_V1.4_{F1705I+GA/SD}$ channels are not sensitive to changes in $[Ca^{2+}]_i$. The dotted lines in panel (**D**) represent $hNa_V1.4$ in 0.5 μM Ca^{2+}. (**E**) Representative steady-state inactivation currents elicited from different holding potentials through $hNa_V1.4_{F1705I+GA/SD}$ channels in the presence and absence of CaM over expression. (**F**) There is a significant ($p<0.004$) hyperpolarizing shift of the inactivation curve by CaM over expression compared to the expression of $hNa_V1.4_{F1705I+GA/SD}$ (in dotted line) alone. Over expression of CaM_{1234} has no significant effect compared with the absence of CaM over expression. (**G**) Representative steady-state inactivation currents elicited from different holding potentials through $hNa_V1.4_{GA/SD}$ channels in the presence and absence of $[Ca^{2+}]_i$. (**H**) Steady-state inactivation of $hNa_V1.4_{GA/SD}$ channel exhibited sensitivity to changes in $[Ca^{2+}]_i$ similar to the wild type rat channel.
doi:10.1371/journal.pone.0081063.g006

the wild type $rNa_V1.4$ in presence of 0.5 μM Ca^{2+} (Figures 4B, 4C and Table 1; $p<0.05$).

IQ-CaM Interaction is Unaffected by $rNa_V1.4_{F1698I}$

The significant alteration in Na^+ current properties demonstrated by $rNa_V1.4_{F1698I}$ suggests the possibility of a disruption of CaM interaction with the IQ motif which is in vicinity of F1698. CaM or CaM_{1234} co-expression does not alter the current kinetics (Figure 5A) or the voltage dependence of activation of $rNa_V1.4_{F1698I}$ (Figure 5C). Similarly, CaM and CaM_{1234} do not affect the activation of wild type rNav1.4 (Table 1). However, co-expression of CaM with $rNa_V1.4_{F1698I}$ significantly shifts channel availability in the hyperpolarizing direction compared to the absence of CaM co-expression (Figures 5B and 5C; $p<0.05$). CaM_{1234} has no effect on the voltage dependence of steady-state inactivation in 0.5 μM $[Ca^{2+}]_i$ (Figure 5C). CaM and CaM_{1234} also have similar effects on wild type rNav1.4 availability (Table 1). The time constants of recovery from inactivated states of $rNa_V1.4_{F1698I}$ are unaffected by over expression of CaM or CaM_{1234} (Table 1). In both species the orthologous myotonia mutations in the CT affect the Ca^{2+} regulation of channel gating. In the rat channel $rNa_V1.4_{F1698I}$ abolished the Ca^{2+} sensitivity observed in the wild type $rNa_V1.4$. In contrast, $hNa_V1.4_{F1705I}$ imparts sensitivity to Ca^{2+} which is absent in wild type $hNa_V1.4$. We postulated that differences in the EFL region of the two channels contribute to the difference in Ca^{2+} response of the orthologous myotonia mutations in the human and rat channels.

EFL Residues Mediate the Differences in Ca^{2+} Regulation

We compared the amino acid sequences in the CT of the rat and human $Na_V1.4$ channels in the EFL and IQ motifs. In the region that includes the EFL (Figure 1A), the amino acids at positions 1613 and 1636 in $hNa_V1.4$ are glycine (G) and alanine (A), and the corresponding residues in $rNa_V1.4$ are serine (S) and aspartic acid (D) respectively (Figure 6A). Position 1613 is within the predicted EFL region whereas residue 1636 is outside the EFL in H1–H2 loop region. We tested the hypothesis that $hNa_V1.4_{F1705I}$ altered channel gating by disruption of Ca^{2+}

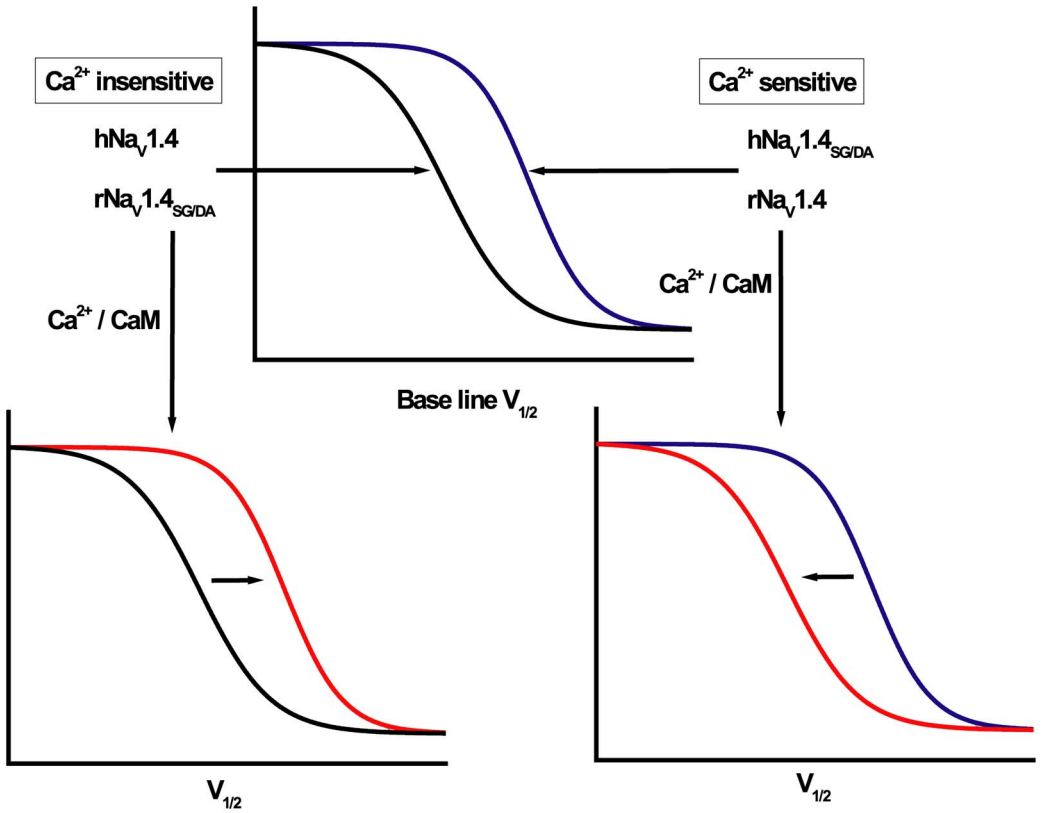

Figure 7. Ca^{2+} sensitivity, inactivation gating and calmodulation. This schematic illustrates the relationship between the Ca^{2+} sensitivity of inactivation gating and the effect of CaM over expression. Channel variants that exhibit shifts in the voltage dependence of inactivation as a function of changes in intracellular $[Ca^{2+}]$ exhibit a depolarized $V_{1/2}$ compared with variants insensitive to Ca^{2+}. The Ca^{2+} sensitivity is associated with the direction of the gating shift induced by CaM over expression. Residues in the EFL are key determinants of the Ca^{2+} sensitivity and effect of CaM over expression on inactivation gating. The red curves in plots indicate steady-state inactivation in the presence of CaM.
doi:10.1371/journal.pone.0081063.g007

sensing through the EFL motif. We generated a triple mutant human channel, containing F1705I and replacing the non-conserved residues in the human EFL with the corresponding amino acids from the rat sequence $hNa_V1.4_{F1705I,G1613S,A1636D}$ ($hNa_V1.4_{F1705I+GS/AD}$). $hNa_V1.4_{F1705I+GS/AD}$ and $hNa_V1.4$ have comparable peak current I–V relationships, and in both cases the voltage dependences of activation were not altered by the absence or presence of 0.5 μM Ca^{2+} (Figures 6B, 6C and Table 1). Similar to $rNa_V1.4_{F1698I}$, steady-state inactivation of $hNa_V1.4_{F1705I+GS/AD}$ was insensitive to changes in the $[Ca^{2+}]_i$ (Figure 6D and Table 1). Thus key residues in the EFL region contributed to the species differences in Ca^{2+} sensitivity of mutations in $Na_V1.4$ that produce myotonia.

Remarkably $hNa_V1.4_{F1705I+GS/AD}$ exhibits CaM regulation that recapitulates that of $rNa_V1.4_{F1698I}$. Over expression of CaM with $hNa_V1.4_{F1705I+GS/AD}$ produces a hyperpolarizing shift in $V_{1/2}$ of steady-state inactivation compared to the mutant channel in the absence of CaM over expression (Figures 6E, 6F and Table 1; $p<0.05$). Similar to $rNa_V1.4_{F1698I}$, CaM_{1234} over expression with $hNa_V1.4_{F1705I+GS/AD}$ does not alter the voltage dependence of steady-state inactivation compared to the mutant channel without CaM_{1234} over expression (Figure 6F and Table 1). The orthologous myotonia mutation on the rat channel background exhibits changes in Ca^{2+}/CaM regulation that are completely different from that of $hNa_V1.4_{F1705I}$. However substituting the EFL residues present in the rat channel into the $hNa_V1.4_{F1705I}$ background is sufficient to recapitulate the Ca^{2+}/CaM regulation exhibited by $rNa_V1.4_{F1698I}$ (Figures 6 and Table 1). This holds true for wild type channels, as mutation of the non-conserved amino acids of the wild type $hNa_V1.4$ EFL to match that of the rat sequence (G1613S and A1636D) reestablished Ca^{2+} and CaM sensitivity of inactivation gating mimicking that of wild type rat $Na_V1.4$ (Figures 6G and 6H, Table 1). Additionally, changing the EFL residues (G and A) from human channel into the wild type rat $Na_V1.4$ ($rNa_V1.4_{SG/DA}$) or mutant $rNa_V1.4_{F1698I}$ ($rNa_V1.4$-$_{F1698I+SG/DA}$) background restored Ca^{2+}/CaM regulation similar to that displayed by $hNa_V1.4$ or $hNa_V1.4_{F1705I}$ respectively (Table 1). Thus the differences in the key amino acids in the EFL region are associated with species-specific differences in Ca^{2+}/CaM regulation of the wild type and mutant, human and rat $Na_V1.4$ channels.

Discussion

Myotonic mutations in $hNa_V1.4$ have been reported to affect Na^+ current inactivation properties. Wu *et al.* demonstrated a destabilization of fast inactivation without significant changes in activation or slow inactivation by the F1705I mutation [7]. However, the mechanism of the change in gating is uncertain as is the role of alteration of Ca^{2+} or CaM modulation of the function of the mutant channel. We have demonstrated that the CT myotonia mutation, $hNa_V1.4_{F1705I}$ slows the I_{Na} decay, depolarizes the voltage dependence of inactivation and augments the window current, effects that may contribute to the cold-induced myotonic phenotype. Notably, $hNa_V1.4_{F1705I}$ imparts intracellular Ca^{2+} sensitivity to inactivation gating, a feature that is distinct from the wild type $hNa_V1.4$. However, the direction of the shift of steady-state inactivation of $hNa_V1.4_{F1705I}$ channels is opposite to the direction of the Ca^{2+}-induced shift observed with cardiac channel, $hNa_V1.5$ [14]. Our data suggest that two key residues in the EFL (Figure 6, Table 1) modify gating of wild type $hNa_V1.4$ and the myotonia mutant $hNa_V1.4_{F1705I}$.

Sodium channel mediated myotonia is characterized electrophysiologically by a delay in inactivation that predisposes to repetitive depolarization and contraction of skeletal muscle after a brief stimulus. Previous studies suggested that a defect in fast inactivation, as in the CT mutant F1705I mutation, was sufficient to produce myotonia [7,37]. Our data shows, that along with a depolarizing shift in steady-state inactivation and slowed I_{Na} decay, reduced intracellular Ca^{2+} levels exaggerate both the depolarizing shift of inactivation (Figures 1D, 1E and 1G) and the slowing of I_{Na} decay of the current (Figures 2A and 2B). It appears that the largest effect of the F1705I mutation is on the voltage dependence and temperature sensitivity of gating but our data suggest that altered $[Ca^{2+}]_i$ sensitivity of the mutant channel potentiates symptoms of myotonia at low temperature. The experiments were designed to test the effects of Ca^{2+} on channel gating and we explored the extremes of the range of concentrations. We do not believe that bulk Ca^{2+} levels ever reach these levels but sub cellular distribution of ion concentrations are heterogeneous and local changes in Ca^{2+} in this range are feasible [38].

Slowing of I_{Na} decay, increased window current, altered voltage dependence of inactivation, along with disruption of Ca^{2+} sensitivity of $hNa_V1.4_{F1705I}$ could explain myotonia, but it is not clear what triggers cold-induced symptoms or why these patients are free from symptoms at normal body temperature. Our study indicates hastening of I_{Na} decay of $hNa_V1.4_{F1705I}$ at normal body temperature eliminates current changes that are associated with the myotonic phenotype. At 37°C, the I_{Na} decay of $hNa_V1.4_{F1705I}$ (at −30 mV) is ~5 times faster than at RT and is nearly identical to the decay rate of wild type $hNa_V1.4$ current at 37°C (Figures 2C and 2D). Additionally, at 37°C, $V_{1/2}$ of steady-state inactivation of $hNa_V1.4_{F1705I}$ significantly shifted ~10 mV in hyperpolarizing direction compared to RT, and is comparable to $V_{1/2}$ of wild type channel at RT (Figure 2E). The temperature dependent shift we observed in the human mutant channel is more than the previously reported ~3 mV temperature dependent shift in steady-state inactivation of native rat skeletal muscle Na channels [39]. Rescue of I_{Na} decay and steady-state inactivation at 37°C could explain why the patients with the F1705I mutation are free from myotonia at normal body temperature. Slowing of deactivation of $hNa_V1.4$ may cause sustained skeletal muscle contraction by delaying repolarization thereby prolonging action potential duration [34]. Differential temperature-induced changes in mutant channel gating; particularly slowing of deactivation resulting in persistent membrane depolarization has been proposed for some $hNa_V1.4$ mutations causing myotonia [40]; however, the F1705I mutation does not alter deactivation [33]. Additionally, it has been suggested that at normal temperatures more wild type channels are activated compared to mutant channels and with lowering of temperature mutant channels dominate membrane excitability [41]. Alternatively changes in temperature may be associated with changes in intracellular $[Ca^{2+}]$ [42] that exaggerate the inactivation gating defects of the mutant channel. We speculate that temperature sensitive changes in intracellular Ca^{2+} could alter cold aggravated myotonia in F1705I mutant muscle.

The biophysical effects of $hNa_V1.4_{F1705I}$ and the orthologous rat mutation $rNa_V1.4_{F1698I}$ are consistent with a key role for the CT in inactivation gating. Residues in and around the EFL motif [21,22] of the CT of $hNa_V1.5$ and $Na_V1.1$ regulate the Ca^{2+} sensitivity of channel gating [14,17,18,23,24,25], which may occur at low levels of free $[Ca^{2+}]$ in the cell [43]. In addition to the EFL, sites in the III–IV linker are involved in Ca^{2+}/CaM mediated regulation of gating [28,29]. We exploited the differences in the EFL sequences and Ca^{2+} sensitivity of inactivation gating of the human and rat orthologous $Na_V1.4$ channels to better understand

the mechanisms of Ca^{2+} modulation of wild type and mutant channels. Inactivation gating of $hNa_V1.4_{F1705I}$ is sensitive to changes in intracellular $[Ca^{2+}]$, in contrast wild type $hNa_V1.4$ exhibits no such sensitivity to Ca^{2+}. The inverse is true for the wild type and mutant rat isoforms of $Na_V1.4$. Mutating the non-conserved amino acids of the $hNa_V1.4$ EFL region to match that of the rat sequence (G1613S and A1636D), abolishes the Ca^{2+} sensitivity of $hNa_V1.4_{F1705I+GS/AD}$ mimicking that of $rNa_V1.4_{F1698I}$. Similarly, mutating the non-conserved amino acids of the wild type $hNa_V1.4$ EFL region to match that of the rat sequence (G1613S and A1636D) restores the Ca^{2+} sensitivity of the channel mimicking that of wild type rat $Na_V1.4$ (Figures 6G, 6H, Table 1). To our knowledge, this is the first report of a mutation in the CT remote from the EFL region that abolishes Ca^{2+} sensitivity of gating of $Na_V1.4$ channels; however, it is not clear that the $rNa_V1.4_{F1698I}$ or $hNa_V1.4_{F1705I}$ has compromised channel gating through a long range conformational effect on the EFL motif. Notably, both rat and human myotonic mutant channels dramatically shift the voltage dependence of inactivation gating in the depolarizing direction. A similar depolarizing shift in inactivation due to a mutation in the CT $hNa_V1.4$ (Q1633E) has been reported, implicating the EFL region of the CT in inactivation gating [9]. Thus it may be that these mutants introduce a significant local structural change in the predicted H5 which in turn influences the neighboring H4 and alters helical interactions in the EFL leading to a disruption of Ca^{2+} sensing. Hydrophobic helical interactions in the cardiac $Na_V1.5$ EFL, particularly H1–H4, appear to stabilize the structure of the proximal CT of the channel which is postulated to be a prerequisite for durable inactivation [44]. Although most of the mutations at the hydrophobic interfaces of the EFL helices shift inactivation in the hyperpolarizing direction, there are important exceptions to this generalization [44].

The mechanism of the Ca^{2+} regulation of gating by residues in the CT is not fully understood and the role of direct Ca^{2+} binding to this region is debated. In fact the crystal structure of a ternary complex of the CT-$hNa_V1.5$, CaM and FHF fails to show Ca^{2+} in the EFL region [27,30]. The structure needs to be viewed in the context of functional studies of the intact channel where mutations of the EFL residues consistently alter the Ca^{2+} sensitivity of $hNa_V1.5$ gating [14,17,18,24,45]. This does not prove that Ca^{2+} is binding to this region; an alternative is that the mutation(s) produce an allosteric change that alters Ca^{2+} sensitivity of gating.

It is interesting that this myotonic mutation in H5 does not affect CaM regulation of the channel. This finding is consistent with previous observations [15] that CaM is an integral part of $Na_V1.4$ and it remains tethered to the mutant channels in all conformations. An alternative explanation is that the IQ-containing H6 interacts with the EFL [24,45] bringing the H5 into physical proximity of the EFL. Thus mutations such as $rNa_V1.4_{F1698I}$ or $hNa_V1.4_{F1705I}$ in H5 could alter the conformation and disrupt Ca^{2+}-sensing but this would have to occur without altering the interaction between CaM and the IQ as myotonic mutant channels of both the species are normally regulated by over expression of CaM (Table 1).

It is clear from our study that intracellular Ca^{2+} has the capacity to regulate some skeletal muscle $Na_V1.4$ isoforms in a manner similar to the cardiac isoform $Na_V1.5$ [14,17,18,24,32], provided the $Na_V1.4$ channel isoforms have proper residues in the EFL sequence. For example, channels with the $rNa_V1.4$ EFL (Figure 6A) or engineered mutant human channels with the orthologous rat residues in the EFL, $hNa_V1.4_{GS/AD}$, are regulated by $[Ca^{2+}]_i$. In contrast, channels with the native human sequence ($hNa_V1.4$) or mutated residues in the EFL ($rNa_V1.4_{SG/DA}$) are insensitive to $[Ca^{2+}]_i$. This study also demonstrates that detailed regulation of inactivation of variants of $Na_V1.$ 4 channels by CaM over expression is determined by the composition of the EFL and the ability of intracellular Ca^{2+} to regulate gating (Figure 7). Irrespective of $Na_V1.4$ channel isoform, CaM mediated regulation of $Na_V1.4$ depends on the EFL residues and $[Ca^{2+}]_i$. The voltage dependence of inactivation gating of the skeletal muscle Na channel variants is either Ca^{2+} sensitive (rat $Na_V1.$ 4, $hNa_V1.4_{GA/DS}$) or insensitive (human $Na_V1.$ 4, $rNa_V1.4_{DS/GA}$). The Ca^{2+} sensitivity is in part determined by the amino acid sequence in the EFL. This sequence divergence is associated with differences in the baseline voltage dependence of inactivation as well as the response to CaM over expression (Figure 7).

Conclusion

The cold aggravated myotonia mutation, $hNa_V1.4_{F1705I}$ in the CT of the skeletal muscle channel remote from the EFL region produces temperature-dependent slowing of current decay and significant destabilization of inactivation, and is associated with a disruption or alteration of Ca^{2+} regulation. Alteration of $[Ca^{2+}]_i$ sensitivity at low temperature could potentiate myotonia symptoms. These changes result in greater Na current availability at depolarized voltages, and thus prolongation of the cellular action potential which is likely to be the proximate cause of myotonia. Moreover the data suggests a mechanism by which drugs that stabilize Na current inactivation may be useful in controlling muscle symptoms. This disease causing mutation and isoform specific amino acid variation in the CT EFL provide important insights into the differences in Ca^{2+} regulation of Na_V1 channels.

Supporting Information

File S1 Includes Methods, Figures S1 – S3 with legends, Table S1, and References.
(DOCX)

Acknowledgments

Dr Tomaselli holds the Michel Mirowski MD Professorship in Cardiology at Johns Hopkins University. Yanli Tian and Victoria Halperin provided technical assistance.

Author Contributions

Conceived and designed the experiments: SB GFT. Performed the experiments: SB. Analyzed the data: SB GFT. Contributed reagents/materials/analysis tools: SB GFT DAD PD. Wrote the paper: SB GFT DAD. Provided technical assistance, design and creation of expression constructs: DAD PD. Did the data interpretation: SB GFT.

References

1. Raja Rayan DL, Hanna MG (2010) Skeletal muscle channelopathies: nondystrophic myotonias and periodic paralysis. Curr Opin Neurol 23: 466–476.
2. Jurkat-Rott K, Holzherr B, Fauler M, Lehmann-Horn F (2010) Sodium channelopathies of skeletal muscle result from gain or loss of function. Pflugers Arch 460: 239–248.
3. Heine R, Pika U, Lehmann-Horn F (1993) A novel SCN4A mutation causing myotonia aggravated by cold and potassium. Hum Mol Genet 2: 1349–1353.
4. Rossignol E, Mathieu J, Thiffault I, Tetreault M, Dicaire MJ, et al. (2007) A novel founder SCN4A mutation causes painful cold-induced myotonia in French-Canadians. Neurology 69: 1937–1941.

5. Schoser BG, Schroder JM, Grimm T, Sternberg D, Kress W (2007) A large German kindred with cold-aggravated myotonia and a heterozygous A1481D mutation in the SCN4A gene. Muscle Nerve 35: 599–606.
6. Bissay V, Keymolen K, Lissens W, Laureys G, Schmedding E, et al. (2011) Late onset painful cold-aggravated myotonia: three families with SCN4A L1436P mutation. Neuromuscul Disord 21: 590–593.
7. Wu FF, Gordon E, Hoffman EP, Cannon SC (2005) A C-terminal skeletal muscle sodium channel mutation associated with myotonia disrupts fast inactivation. J Physiol 565: 371–380.
8. Miller TM, Dias da Silva MR, Miller HA, Kwiecinski H, Mendell JR, et al. (2004) Correlating phenotype and genotype in the periodic paralyses. Neurology 63: 1647–1655.
9. Kubota T, Kinoshita M, Sasaki R, Aoike F, Takahashi MP, et al. (2009) New mutation of the Na channel in the severe form of potassium-aggravated myotonia. Muscle Nerve 39: 666–673.
10. Deschenes I, Neyroud N, DiSilvestre D, Marban E, Yue DT, et al. (2002) Isoform-specific modulation of voltage-gated Na(+) channels by calmodulin. Circ Res 90: E49–57.
11. Kim J, Ghosh S, Liu H, Tateyama M, Kass RS, et al. (2004) Calmodulin mediates Ca2+ sensitivity of sodium channels. J Biol Chem 279: 45004–45012.
12. Mantegazza M, Yu FH, Catterall WA, Scheuer T (2001) Role of the C-terminal domain in inactivation of brain and cardiac sodium channels. Proc Natl Acad Sci U S A 98: 15348–15353.
13. Motoike HK, Liu H, Glaaser IW, Yang AS, Tateyama M, et al. (2004) The Na+ channel inactivation gate is a molecular complex: a novel role of the COOH-terminal domain. J Gen Physiol 123: 155–165.
14. Biswas S, DiSilvestre D, Tian Y, Halperin VL, Tomaselli GF (2009) Calcium-mediated dual-mode regulation of cardiac sodium channel gating. Circ Res 104: 870–878.
15. Biswas S, Deschenes I, Disilvestre D, Tian Y, Halperin VL, et al. (2008) Calmodulin regulation of Nav1.4 current: role of binding to the carboxyl terminus. J Gen Physiol 131: 197–209.
16. Young KA, Caldwell JH (2005) Modulation of skeletal and cardiac voltage-gated sodium channels by calmodulin. J Physiol 565: 349–370.
17. Wingo TL, Shah VN, Anderson ME, Lybrand TP, Chazin WJ, et al. (2004) An EF-hand in the sodium channel couples intracellular calcium to cardiac excitability. Nat Struct Mol Biol 11: 219–225.
18. Shah VN, Wingo TL, Weiss KL, Williams CK, Balser JR, et al. (2006) Calcium-dependent regulation of the voltage-gated sodium channel hH1: intrinsic and extrinsic sensors use a common molecular switch. Proc Natl Acad Sci U S A 103: 3592–3597.
19. Erickson MG, Alseikhan BA, Peterson BZ, Yue DT (2001) Preassociation of calmodulin with voltage-gated Ca(2+) channels revealed by FRET in single living cells. Neuron 31: 973–985.
20. Mori MX, Erickson MG, Yue DT (2004) Functional stoichiometry and local enrichment of calmodulin interacting with Ca2+ channels. Science 304: 432–435.
21. Babitch J (1990) Channel hands. Nature 346: 321–322.
22. Cormier JW, Rivolta I, Tateyama M, Yang AS, Kass RS (2002) Secondary structure of the human cardiac Na+ channel C terminus: evidence for a role of helical structures in modulation of channel inactivation. J Biol Chem 277: 9233–9241.
23. Casini S, Verkerk AO, van Borren MM, van Ginneken AC, Veldkamp MW, et al. (2009) Intracellular calcium modulation of voltage-gated sodium channels in ventricular myocytes. Cardiovasc Res 81: 72–81.
24. Chagot B, Potet F, Balser JR, Chazin WJ (2009) Solution NMR structure of the C-terminal EF-hand domain of human cardiac sodium channel NaV1.5. J Biol Chem 284: 6436–6445.
25. Gaudioso C, Carlier E, Youssouf F, Clare JJ, Debanne D, et al. (2011) Calmodulin and calcium differentially regulate the neuronal Nav1.1 voltage-dependent sodium channel. Biochem Biophys Res Commun 411: 329–334.
26. Miloushev VZ, Levine JA, Arbing MA, Hunt JF, Pitt GS, et al. (2009) Solution structure of the NaV1.2 C-terminal EF-hand domain. J Biol Chem 284: 6446–6454.
27. Wang C, Chung BC, Yan H, Lee SY, Pitt GS (2012) Crystal structure of the ternary complex of a NaV C-terminal domain, a fibroblast growth factor homologous factor, and calmodulin. Structure 20: 1167–1176.
28. Potet F, Chagot B, Anghelescu M, Viswanathan PC, Stepanovic SZ, et al. (2009) Functional Interactions between Distinct Sodium Channel Cytoplasmic Domains through the Action of Calmodulin. J Biol Chem 284: 8846–8854.
29. Sarhan MF, Van Petegem F, Ahern CA (2009) A double tyrosine motif in the cardiac sodium channel domain III–IV linker couples calcium-dependent calmodulin binding to inactivation gating. J Biol Chem 284: 33265–33274.
30. Sarhan MF, Tung CC, Van Petegem F, Ahern CA (2012) Crystallographic basis for calcium regulation of sodium channels. Proc Natl Acad Sci U S A 109: 3558–3563.
31. Bers DM, Patton CW, Nuccitelli R (1994) A practical guide to the preparation of Ca2+ buffers. Methods Cell Biol 40: 3–29.
32. Tan HL, Kupershmidt S, Zhang R, Stepanovic S, Roden DM, et al. (2002) A calcium sensor in the sodium channel modulates cardiac excitability. Nature 415: 442–447.
33. Groome JR, Larsen MF, Coonts A (2008) Differential effects of paramyotonia congenita mutations F1473S and F1705I on sodium channel gating. Channels (Austin) 2: 39–50.
34. Featherstone DE, Fujimoto E, Ruben PC (1998) A defect in skeletal muscle sodium channel deactivation exacerbates hyperexcitability in human paramyotonia congenita. J Physiol 506 (Pt 3): 627–638.
35. Plassart-Schiess E, Lhuillier L, George AL, Jr., Fontaine B, Tabti N (1998) Functional expression of the Ile693Thr Na+ channel mutation associated with paramyotonia congenita in a human cell line. J Physiol 507 (Pt 3): 721–727.
36. Richmond JE, Featherstone DE, Ruben PC (1997) Human Na+ channel fast and slow inactivation in paramyotonia congenita mutants expressed in Xenopus laevis oocytes. J Physiol 499 (Pt 3): 589–600.
37. Green DS, George AL, Jr., Cannon SC (1998) Human sodium channel gating defects caused by missense mutations in S6 segments associated with myotonia: S804F and V1293I. J Physiol 510 (Pt 3): 685–694.
38. Eisenberg B (2013) Interacting Ions in Biophysics: Real is not Ideal. Biophys J 104: 1849–1866.
39. Ruff RL (1999) Effects of temperature on slow and fast inactivation of rat skeletal muscle Na(+) channels. Am J Physiol 277: C937–947.
40. Dice MS, Abbruzzese JL, Wheeler JT, Groome JR, Fujimoto E, et al. (2004) Temperature-sensitive defects in paramyotonia congenita mutants R1448C and T1313M. Muscle Nerve 30: 277–288.
41. Mitrovic N, George AL, Jr., Rudel R, Lehmann-Horn F, Lerche H (1999) Mutant channels contribute <50% to Na+ current in paramyotonia congenita muscle. Brain 122 (Pt 6): 1085–1092.
42. Bruton JD, Aydin J, Yamada T, Shabalina IG, Ivarsson N, et al. (2010) Increased fatigue resistance linked to Ca2+-stimulated mitochondrial biogenesis in muscle fibres of cold-acclimated mice. J Physiol 588: 4275–4288.
43. Van Petegem F, Lobo PA, Ahern CA (2012) Seeing the forest through the trees: towards a unified view on physiological calcium regulation of voltage-gated sodium channels. Biophys J 103: 2243–2251.
44. Glaaser IW, Bankston JR, Liu H, Tateyama M, Kass RS (2006) A carboxyl-terminal hydrophobic interface is critical to sodium channel function. Relevance to inherited disorders. J Biol Chem 281: 24015–24023.
45. Glaaser IW, Osteen JD, Puckerin A, Sampson KJ, Jin X, et al. (2012) Perturbation of sodium channel structure by an inherited Long QT Syndrome mutation. Nat Commun 3: 706.